Research Resource: Transcriptional Profiling Reveals Different Pseudohypoxic Signatures in SDHB and VHL-Related Pheochromocytomas

Elena López-Jiménez, Gonzalo Gómez-López, L. Javier Leandro-García, Iván Muñoz, Francesca Schiavi, Cristina Montero-Conde, Aguirre A. de Cubas, Ricardo Ramires, Iñigo Landa, Susanna Leskelä, Agnieszka Maliszewska, Lucía Inglada-Pérez, Leticia de la Vega, Cristina Rodríguez-Antona, Rocío Letón, Carmen Bernal, José M. de Campos, Cristina Diez-Tascón, Mario F. Fraga, Cesar Boullosa, David G. Pisano, Giuseppe Opocher, Mercedes Robledo, and Alberto Cascón

Hereditary Endocrine Cancer Group (E.L.-J., L.J.L.-G., C.M.-C., A.A.d.C., I.L., S.L., A.M., L.I.-P., L.d.l.V., C.R.-A., R.L., M.R., A.C.), Structural Biology and Biocomputing Programme (G.G.-L., C.B., D.G.P.), and Human Genetics Group (I.M., R.R.), Spanish National Cancer Research Centre, 28029 Madrid, Spain; Familial Cancer Clinic (F.S., G.O.), Veneto Institute of Oncology, 35128 Padua, Italy; ISCIII Center for Biomedical Research on Rare Diseases (C.R.-A., M.R., A.C.) and Endocrinology and Nutrition Service (C.B.), Hospital 12 de Octubre, C Madrid, Spain; Neurosurgery Department (J.M.d.C.), Fundación Jiménez Díaz, 28040 Madrid, Spain; Banco de Tumores (C.D.-T.), Complejo Hospitalario de León, 24008 Leon, Spain; Department of Immunology and Oncology (M.F.F.), National Center for Biotechnology, Centro Nacional de Biotecnología-Consejo Superior de Investigaciones Científicas, Cantoblanco, 28049 Madrid, Spain; and Department of Medical and Surgical Sciences (G.O.), University of Padua, 35128 Padua, Italy

The six major genes involved in hereditary susceptibility for pheochromocytoma (PCC)/paraganglioma (PGL) (*RET*, *VHL*, *NF1*, *SDHB*, *SDHC*, and *SDHD*) have been recently integrated into the same neuronal apoptotic pathway where mutations in any of these genes lead to cell death. In this model, prolyl hydroxylase 3 (EglN3) abrogation plays a pivotal role, but the molecular mechanisms underlying its inactivation are currently unknown. The aim of the study was to decipher specific alterations associated with the different genetic classes of PCCs/PGLs. With this purpose, 84 genetically characterized tumors were analyzed by means of transcriptional profiling. The analysis revealed a hypoxia-inducible factor (HIF)-related signature common to succinate dehydrogenase (SDH) and von Hippel-Lindau (VHL) tumors, that differentiated them from RET and neurofibromatosis type 1 cases. Both canonical HIF-1α and HIF-2α target genes were overexpressed in the SDH/VHL cluster, suggesting that a global HIF deregulation accounts for this common profile. Nevertheless, when we compared VHL tumors with SDHB cases, which often exhibit a malignant behavior, we found that HIF-1α target genes showed a predominant activation in the VHL PCCs. Expression data from 67 HIF target genes was sufficient to cluster SDHB and VHL tumors into two different groups, demonstrating different pseudohypoxic signatures. In addition, VHL-mutated tumors showed an unexpected overexpression of EglN3 mRNA that did not lead to significantly different EglN3 protein levels. These findings pave the way for more specific therapeutic approaches for malignant PCCs/PGLs management based on the patient's genetic alteration. **(*Molecular Endocrinology* 24: 2382–2391, 2010)**

ISSN Print 0888-8809 ISSN Online 1944-9917
Printed in U.S.A.

doi: 10.1210/me.2010-0256 Received June 30, 2010. Accepted September 30, 2010.
First Published Online October 27, 2010

Abbreviations: BNIP3, BCL2/adenovirus E1B 19-kDa protein-interacting protein 3; Cy, cyanine; EglN3, prolyl hydroxylase 3; FDR, false discovery rate; FFPE, formalin-fixed paraffin-embedded; FPCC, familial PCC; GSEA, gene set enrichment analysis; HIF, hypoxia-inducible factor; MSP, methylation-specific polymerase chain reaction; NF1, neurofibromatosis type 1; NOM, nomina; PCC, pheochromocytoma; PGL, paraganglioma; SDH, succinate dehydrogenase; VHL, von Hippel-Lindau; VEGF, vascular endothelial growth factor.

Pheochromocytomas (PCCs) and paragangliomas (PGLs) are rare neuroendocrine tumors that arise from the adrenal medulla and from extraadrenal paraganglia distributed along the paravertebral axis or located in the skull base and neck, respectively. PCCs and PGLs mainly occur as sporadic tumors but can be associated with three well-known hereditary neuroendocrine syndromes: multiple endocrine neoplasia type 2 caused by germline mutations in the *RET* proto-oncogene; von Hippel-Lindau (VHL) disease, associated with mutations in the *VHL* tumor-suppressor gene; and neurofibromatosis type 1 (NF1) caused by mutations in *NF1*. In addition, heterozygous germline mutations in three of the four genes encoding the succinate dehydrogenase (SDH) enzyme (*SDHB*, *SDHC*, and *SDHD*) are also involved in the development of the disease. This "housekeeping" enzyme participates both in the Krebs cycle and in the electron-transport chain, and recently, the fourth subunit of this protein (SDHA) and a SDHA-interacting protein [succinate dehydrogenase complex assembly factor 2 (SDHAF2)] have been found to be occasionally altered in PGL patients (1, 2). Finally, the transmembrane-encoding gene *TMEM127*, a negative regulator of mammalian target of rapamycin, has also been reported as a new PCC susceptibility gene (3).

Recently, it was described that the six major genes involved in PCC/PGL susceptibility (*RET*, *VHL*, *NF1*, *SDHB*, *SDHC*, and *SDHD*) can be integrated into the same neuronal apoptotic pathway, where mutations in any of these genes lead to deregulation of nerve growth factor signaling and attenuation of the consequent cell death (4). Although *RET*, *NF1*, and *VHL* mutations abrogate the proapoptotic transcription factor c-Jun by means of JunB induction, *SDH* inactivation leads to the accumulation of succinate that inhibits prolyl hydroxylase 3 (PHD3, also called EglN3)-induced apoptosis (4). Therefore, in this model, EglN3-induced apoptosis must be inhibited for PCC/PGL development to occur. Moreover, another downstream effector in this pathway, KIF1B-β, was recently reported to be altered in PCCs and neuroblastomas (5).

Besides the impressive advances that classical genetic studies of this disease have made during the past 10 yr, new genomic strategies, such as expression profiling, have thrown light on the different biological processes involved in PCC/PGL development (6–8). Thus, a transcriptional profiling study performed in a large series of PCCs/PGLs revealed two dominant expression groups: one included all VHL and SDH tumors, and the other clustered the PCCs carrying RET and NF1 mutations (6). The predominant hypoxic-angiogenic expression features observed in the SDH/VHL cluster linked these genetically different tumors by an autoregulatory loop. Although in VHL tumors hypoxia-inducible factor (HIF)-1α contributes to the attenuation of SDHB levels resulting in SDH inhibition, in SDH tumors inactivation of the mitochondrial complex II and subsequent succinate accumulation blocks HIF-1α degradation by EglN3 inhibition (6). A recent study also found this common angiogenic profile in SDH and VHL tumors and described that, despite both genetic classes demonstrated a decrease in electron transport protein expression and activity, the stimulation of glycolysis was only observed in VHL specimens (8). Although the apoptotic and the hypoxic pathways link SDHB and VHL tumors, little is known about the transcriptional differences between these genetically similar classes that have very different clinical outcomes (SDHB-related tumors are significantly more aggressive than those arising in VHL patients). In the present study, we found that these genetic PCC/PGL classes can be distinguished by means of gene expression profiling and that EglN3 mRNA was exclusively overexpressed in VHL tumors.

Results

Genetic characteristics of the tumors

Germline (42 cases) or somatic (five cases) genetic alterations were found in 47 tumors involving: *RET* (15; one somatic), *VHL* (15; four somatic), *SDHB* (eight), *SDHC* (one), *SDHD* (four), and four previously diagnosed NF1 cases. This information was used to establish the genetic classes used in subsequent analyses. The remaining samples, without mutations in any of the six major susceptibility genes, were classified as sporadic (31 cases), with the exception of six tumors classified as familial PCC (FPCC) cases, because of the presence of familial antecedents of adrenal PCC. All *SDHD* and *SDHC* cases, but none of the *SDHB* tumors, were located in the head and neck region.

Expression profiling related to genetic background

A full listing of the microarray results has been deposited in the National Center for Biotechnology Information Gene Expression Omnibus database under the accession no. GSE19422. Unsupervised and consensus clustering analysis, performed using the 2621 clones that remained after the preprocessing step, revealed a great homogeneity among cases sharing an alteration in the same gene (Fig. 1). Two main clusters were found, mainly defined by SDH/VHL and by RET/NF1 specimen profiles, respectively. The FPCC cases were spread along the RET/NF1 cluster, similarly to the majority of the sporadic tumors. Both adrenal and extraadrenal tumors were represented in the two clusters, whereas the head and neck tumors were all grouped within the SDH/VHL branch. Neither the mutation type nor the origin of the alteration (somatic or germline) had an evident influence on the clustering. A second unsupervised cluster-

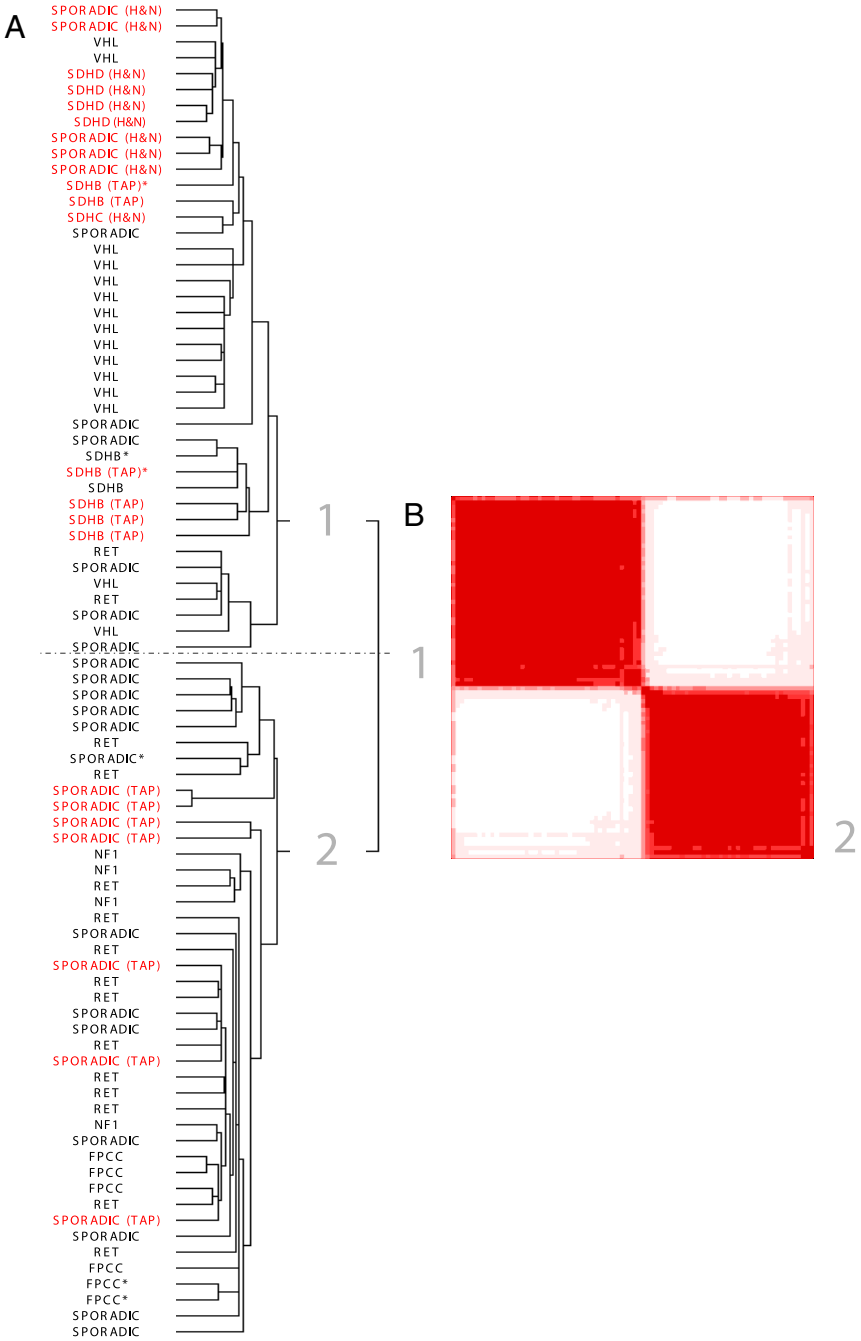

FIG. 1. A, Unsupervised clustering of 84 PCCs, either with extraadrenal (*red letters*) or adrenal location (*black letters*), named according to their genetic background: RET (mutation in *RET*), VHL (mutation in *VHL*), SDHB (mutation in *SDHB*), SDHC (mutation in *SDHC*), SDHD (mutation in *SDHD*), NF1 (from patients with NF1), SPORADIC (apparently sporadic cases without mutations), and FPCC (familial cases without mutations). H&N, Head and neck tumors; TAP, thoracic/abdominal/pelvic tumors. *An asterisk* indicates malignant tumors. B, Consensus matrix that verifies the reliability of the two major clusters (1 and 2) obtained in the unsupervised clustering.

ing performed with the expression data from a list of ranked HIF target genes (see *Materials and Methods*) correctly classified all tumors into the two major branches previously obtained, with the exception of two samples (Supplemental Fig. 1, published on The Endocrine Society's Journals Online web site at http://mend.endojournals.org). One hundred and forty-one genes were used for this second clustering, after discarding genes that exhibited flat patterns across the sample set (SD = 0.8). Among the downstream HIF targets, mainly overexpressed in SDH/VHL tumors, we found genes responsible for the Warburg effect (regulating glucose uptake and metabolism) and angiogenesis (*VEGF* and *PDGF*). HIF-1α mRNA showed no differences between both clusters, but we found a striking significant overexpression of *HIF-2α* (*EPAS1*) in SDH/VHL tumors [3.1-fold; false discovery rate (FDR) 1.00E-07]. Although HIF-1α protein expression showed no differences between the main clusters, we found that HIF-2α expression was higher in SDH/VHL tumors, especially in SDH-related cases (Supplemental Fig. 2).

Transcriptional profile of SDH/VHL tumors

Supervised analysis of representative classes from the two major clusters (SDH/VHL and RET/NF1) revealed 1118 clones significantly differentially expressed between both groups (FDR $<$ 0.05) (Supplemental Table 1). The gene set enrichment analysis (GSEA) test, focused on the different biological processes occurring in SDH/VHL samples compared with RET/NF1, showed seven pathways overrepresented in the SDH/VHL tumor group [nominal (NOM), $P < 0.05$)] (Supplemental Table 2). These included the neural development Notch pathway (both in the BioCarta and the Kyoto Encyclopedia of Genes and Genomes predictions), another Notch-related pathway (PS1PATHWAY), and the hypoxic HIF and vascular endothelial growth factor (VEGF) pathways. Among the genes differentially expressed between SDH/VHL and RET/NF1 clusters (FDR $<$ 0.05), 48 genes were identified as HIF target genes, because they were found in the set of genes included in the ranked list of HIF target genes.

Differential gene expression between VHL and SDHB tumors

Despite their common transcriptional profile, VHL and SDH tumors show very different clinical characteris-

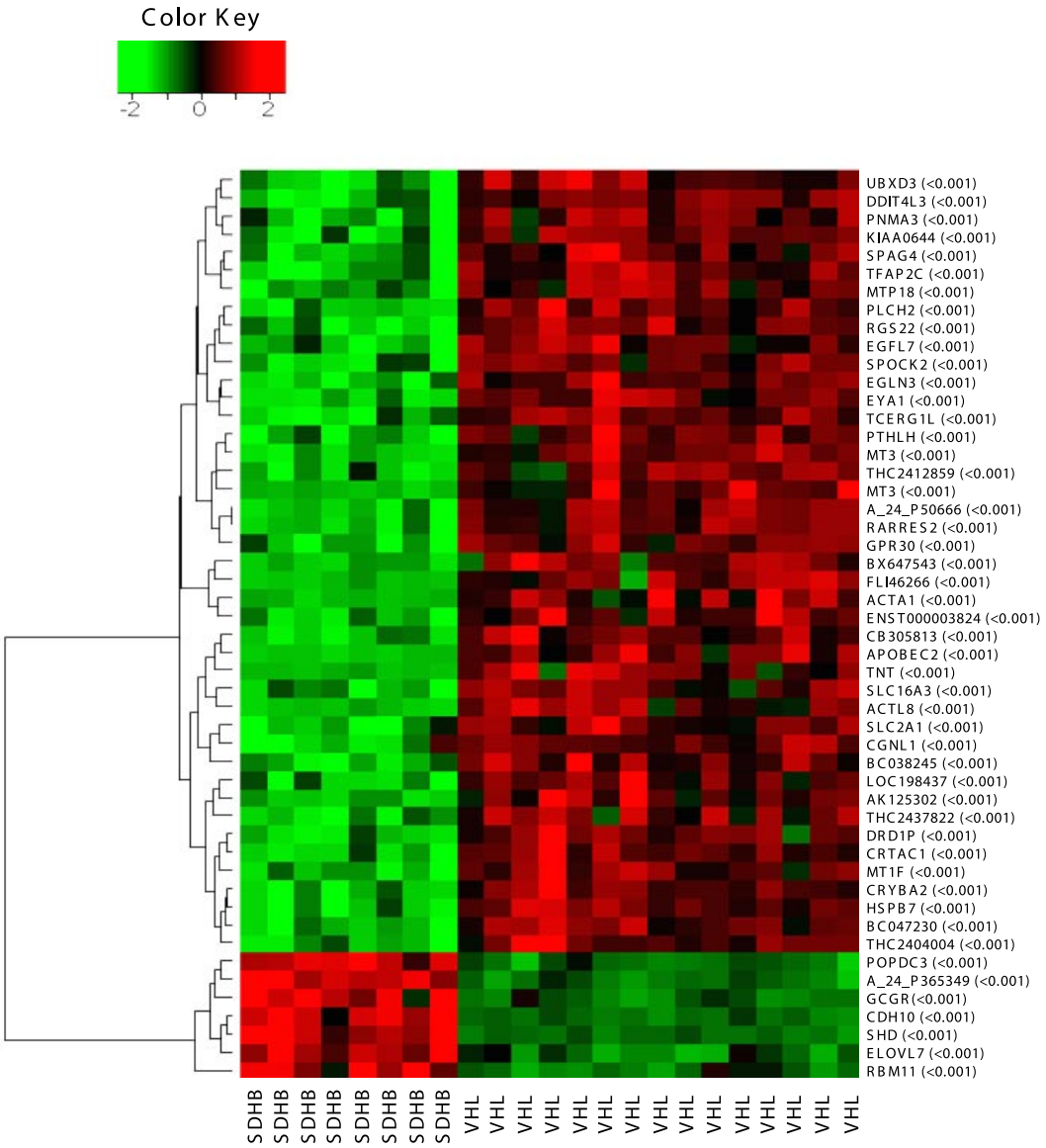

FIG. 2. Heat map showing the 50 top clones (represented in the *rows*) differentially expressed (FDR < 0.05) in the supervised comparison of VHL and SDHB tumors (represented in the *columns*). *Color bar*, *Green* and *red colors* represent relative under- and overexpression of more than or equal to 2-fold, respectively.

tics. For example, SDHB-related tumors usually develop as extraadrenal masses with a high risk of malignancy (50%), whereas VHL tumors are mainly adrenal and malignancy is uncommon (5%) (9–11). Thus, we performed a supervised comparison of VHL and SDHB tumors, which were the most representative classes of the SDH/VHL cluster, to identify molecular patterns underlying this different clinical behavior. The supervised test performed to find transcriptional differences between VHL and SDHB tumors revealed 886 clones, corresponding to 782 genes, significantly differentially expressed between both tumor classes (FDR < 0.05) (Fig. 2 and Supplemental Table 3). Comparison of these two genetic classes through GSEA showed several BioCarta pathways overrepresented in one of the two classes (Supplemental Table 4). Briefly, we found overrepresentation of genes belonging to several TNF-related (TNFR1, TNFR2, HIVNEF, SODD, and STRESS) and apoptotic (D4GDI and DEATH) pathways in VHL cases, and overrepresentation of genes included in three actin organization pathways (INTEGRIN, EPHA4, and CDC42RAC) in SDHB tumors (NOM $P < 0.05$). A high number of HIF target genes (n = 41) was differentially expressed between VHL and SDHB tumors; surprisingly, 17 of them were already found differentially expressed in the SDH/VHL cluster *vs.* the RET/NF1 (Fig. 3A). Because the hypoxia-related genes were differentially expressed across both genetic classes, we wondered whether HIF target genes alone could also distinguish between them. Unsupervised clustering of SDHB and VHL tumors using expression data

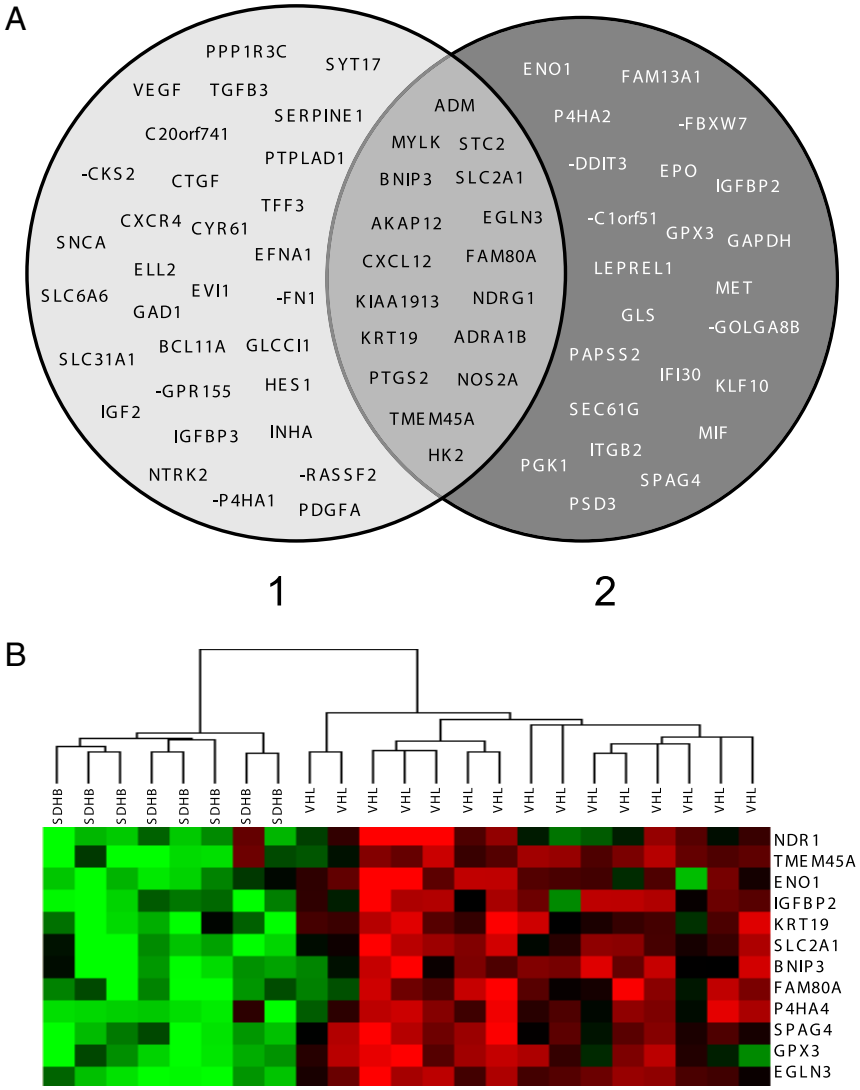

FIG. 3. A, Diagram showing the list of HIF target genes differentially expressed in two different supervised comparisons. 1, VHL-SDH tumor class compared with RET-NF1; 2, VHL compared with SDHB cases. For a given gene, a *minus sign* indicates down-regulation for each respective tumor class, VHL-SDH and VHL. B, Heat map produced by unsupervised clustering of 15 VHL cases and eight SDHB cases, using 12 HIF target genes.

from HIF target genes classified the tumors into two different groups, according to their genetic background, demonstrating a different hypoxic signature. After discarding those genes that exhibited flat patterns across the sample set (SD = 0.8), 67 genes were used for the clustering. In fact, of these 67 HIF target genes, gene expression data from the 12 top-ranked genes was sufficient to distinguish between both tumor types (Fig. 3B), and among them, we found canonical HIF-1α genes like *BNIP3* and *SLC2A1* (*GLUT1*) (12, 13).

Validation of the differentially expressed genes

Quantitative RT-PCR was initially performed using total RNA from eight VHL and five SDHB tumors previously hybridized. A second validation step was performed in an alternative series of 13 formalin-fixed paraffin-embedded (FFPE) tumors: seven VHL and six SDHB cases (Fig. 4A). The validation was carried out for six genes significantly differentially expressed between VHL and SDHB tumors selected from the top-ranked list of genes of the supervised analysis. In both tumor sets, we found a significantly different expression between VHL and SDHB classes that validated the result obtained in the microarray analysis.

Immunohistochemical detection of EglN3 protein

All positive cases assessed showed a cytoplasmic staining pattern. Half (4/8) of the VHL tumors showed a positive staining for EglN3. In addition, 66.7% (6/9) of SDHB cases, 29% (7/24) of RET cases, and 100% of SDHD tumors (4/4) were positive for immunohistochemical detection of EglN3 (Fig. 4B). Finally, 55.6% (5/9) of sporadic PCCs and all normal adrenal tissues included in the tissue arrays also resulted positive for EglN3.

Analysis of Egln3 promoter methylation

Although low levels of EglN3 in non-VHL hereditary PCCs (RET, NF1, and SDH) may be explained by an alteration in one of the PCC susceptibility genes, sporadic tumors do not have any known alteration in the developmental apoptotic pathway. Thus, we assessed the *EglN3* promoter methylation status in sporadic cases. We did not find promoter methylation in the CpG islands analyzed in the 31 sporadic cases studied.

Discussion

The transcriptional clustering observed in PCC depends on the hypoxic signature

Unsupervised profiling of 84 PCCs/PGLs revealed two major groups of tumors defined by their genetic mutation/background: SDH/VHL and RET/NF1 (Fig. 1). Our results showed a hypoxic transcriptional signature (represented by HIF and VEGF pathways) in the SDH/VHL cluster (Supplemental Table 2) that confirmed a common angiogenesis/hypoxia profile typical of VHL dysfunction

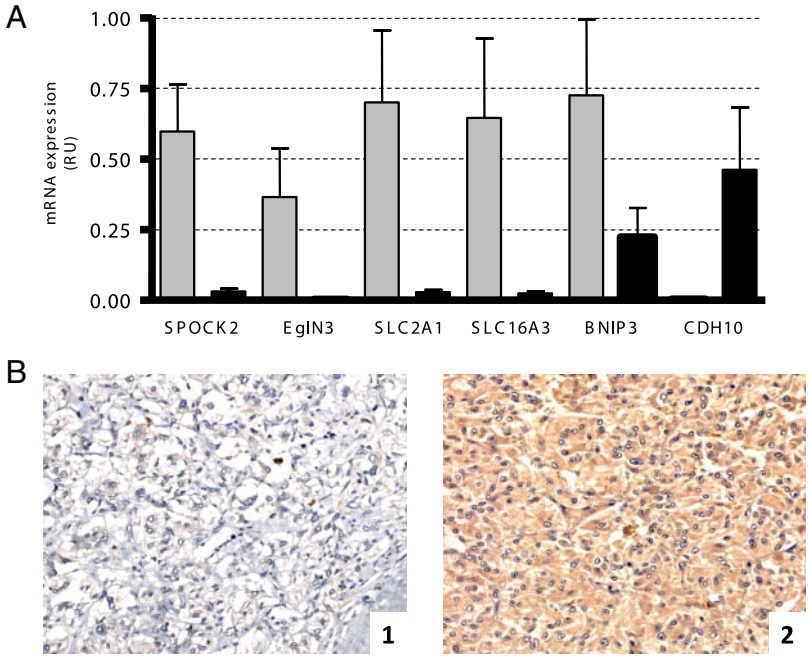

FIG. 4. A, Quantitative real-time RT-PCR analysis of six genes significantly differentially expressed between VHL tumors (*gray bars*) and SDHB FFPE tumors (*black bars*): five overexpressed (*SPOCK2*, *EglN3*, *SLC2A1*, *SLC16A3*, and *BNIP3*) and one underexpressed (*CDH10*) in VHL tumors. The analysis of each gene was performed in triplicate, and relative mRNA levels (RU) were determined using *HPRT1* as internal control. B, Immunohistochemical negative (1) and positive (2) staining of Egln3 carried out in two VHL tumors.

(6). In addition, two Notch-related pathways were overrepresented in the SDH/VHL samples. This agrees with the hypoxic signature, because there is a cross talk between hypoxia and Notch signaling where the Notch intracellular domain directly interacts with the HIF-1α (14). Unsupervised clustering using HIF target genes revealed the same transcriptional distinction between the two major clusters (Supplemental Fig. 1). The significant overexpression of *HIF-2α* in SDH/VHL tumors was especially interesting, consistent with previously reported studies (7, 8). In addition, *NOX4*, critical for HIF-2α transcriptional activity (15), and *VEGF*, a HIF-2α-specific target gene in VHL-defective renal cell carcinoma cells (12, 16), were both up-regulated in SDH/VHL tumors. Thus, it seems that HIF-2α deregulation has an important role in the hypoxic SDH/VHL transcriptional profile.

Expression profiling distinguishes between VHL and SDHB tumors

We found a foreseeable down-regulation of *SDHB* mRNA only in SDHB compared with VHL PCCs (5.1-fold; FDR $<$ 0.003), suggesting that the attenuation of SDHB protein levels reported in VHL tumors (6) is posttranscriptional, which is in agreement with previously reported findings (8). Interestingly, several TNF apoptotic pathways were augmented in VHL tumors, whereas three actin-related pathways involved in cell-cell interaction and migration were overrepresented in the SDHB group. Overexpression of cell-adhesion related genes had been previously described in *SDHB*-silenced cells (17). The significant overexpression of the neuronal cell adhesion gene *CDH10* (cadherin 10) in SDHB tumors compared not only with VHL (15.0-fold; FDR $<$ 0.002), but also to any other genetic class (FDR $<$ 0.001) is noteworthy. Adhesion molecules, including cadherins, play an important role in cell migration and metastasis, so a differential expression of these molecules in potentially malignant tumors may help to define future therapeutic targets.

HIF-1α/HIF-2α deregulation differentiates VHL from SDHB tumors

Differences in expression of HIF-1 and HIF-2α and target genes have been recently detected in VHL and SDH PCCs, suggesting specific mechanisms of HIF deregulation in both tumor types (8, 16). Despite finding a higher HIF-2α protein expression in SDH tumors, we did not find significant differences either in HIF-2α or VEGF mRNA expression between VHL and SDHB tumors, suggesting that HIF-1α deregulation accounts for this distinction. In agreement with these findings, expression of genes involved in HIF-1α-dependent glycolysis (such as *SLC2A1*) has been recently described to be specifically linked to VHL PCCs (8). Transcriptional induction of HIF targets is profoundly influenced by cell type, and the relative HIF-1α/HIF-2α protein abundance modulates the clinical phenotype of VHL (18). Our findings suggest that both transcription factors are deregulated in VHL PCCs, with a predominant activation of HIF-1α target genes that leads to a molecular distinction from SDH-mutated tumors. Moreover, it was especially striking that *EglN3* mRNA levels were up-regulated in VHL tumors compared with SDHB tumors (16.6-fold; FDR $<$ 0.002). It has been reported that up-regulation of *EglN3* can be driven by both HIF transcription factors, with HIF-2α being the stronger activator (19). However, our results suggest that HIF-1α may have a more important role in the regulation of *EglN3* expression, at least in VHL-related PCC.

EglN3 mRNA overexpression is exclusive of VHL-mutated PCCs

Significant EglN3 mRNA overexpression was found in VHL tumors compared not only with SDHB tumors but

also with any other tumor class or normal tissue hybridized (FDR < 0.005) (data not shown). This overexpression of *EglN3* had been previously described in VHL tumors compared with RET cases (7). *EglN3* is a HIF-α target gene that encodes one member of the EglN family of prolyl hydroxylases, consisting of EglN1, EglN2, and EglN3. These proteins modify specific prolyl residues of HIF-α for its ubiquitination by the VHL ubiquitin ligase complex and subsequent degradation (20). Although all three members of the EglN family can hydroxylate HIF-1α *in vitro* (21), it was suggested that EglN1 is the critical oxygen sensor, regulating oxygen-dependent HIF-1α degradation in normoxia and after a short exposure to hypoxia (22). In our study, EglN3 was the only up-regulated EglN member in VHL tumors. In addition, EglN3 plays a role in skeletal muscle differentiation, regulation of nuclear factor κB, and contributes to cellular homeostasis and apoptotic cell death (4, 23–25). Regarding the latter function, *VHL* mutations can promote inhibition of EglN3 expression through the JunB cascade, because all disease-associated pVHL mutants fail to down-regulate JunB (4). Nevertheless, *VHL* mutations can also lead to EglN3 accumulation and, subsequently, promote neuronal apoptosis by the deregulation of HIF-α (21). This deregulation of HIF-α has been described for VHL type 1 mutant cells, whereas type 2 mutant cells, related to PCC development, retain some ability to regulate HIF-α and therefore to maintain lower levels of EglN3 (21). Moreover, VHL type 2C alleles, which are associated to FPCC, appear to be essentially wild type with respect to HIF (21). In the present study, all VHL-PCCs, including a specimen with a well-known type 2C mutation (p.Val84Leu), expressed high EglN3 mRNA levels compared with normal adrenal tissue. Moreover, up-regulation of genes related to glucose metabolism (*i.e.* canonical HIF targets like *SLC2A1*) was also seen in all VHL-related tumors from our series (n =15) compared with non-VHL tumors (n = 69) (FDR < 0.005) (data not shown). Thus, it seems that the VHL-PCC up-regulation of *EglN3* in our series is due to deregulation of HIF-1α, specifically associated with *VHL* mutations. Therefore, EglN3 expression, barely detected in normal adrenal tissues, is induced in hypoxic VHL PCCs and does not seem to have a negative feedback role in the activation of HIF-1α. Nevertheless, immunostaining of EglN3 did not show differences at the protein level among the genetic classes of PCC/PGL (Fig. 4B). Regarding this, overexpression of EglN3 mRNA has been reported in renal cell carcinoma cell lines with mutations in *VHL*, but immunohistochemical assessment failed to reveal differences in protein levels between VHL- and non-VHL renal tumors (26). In addition, a recent study reports that an 100-fold Egln3 mRNA overexpression obtained from mice podocytes lacking *VHL* does not lead to such great differences at the protein level (27). These findings are in agreement with our results, which probably indicates that VHL/HIF alone does not regulate the expression of the EglN3 gene, and a still unknown posttranscriptional mechanism must be involved in the regulation of EglN3 mRNA in VHL PCCs. Inactivation of *EglN3* by promoter hypermethylation was recently described in plasma cell neoplasia (28); nevertheless, our data suggest that methylation of the upstream CpG island of this gene is not a frequent event in sporadic tumors; therefore, the mechanisms responsible for the lack of EglN3 expression observed in these PCCs remain to be found.

BCL2/adenovirus E1B 19-kDa protein-interacting protein 3 (BNIP3) overexpression is specifically linked to VHL mutations in PCC

Another HIF target gene differentially expressed in VHL PCCs compared with any other tumor class included in the present study was *BNIP3*. BNIP3 is a pro-apoptotic protein, up-regulated by p53 and HIF-1α and negatively regulated by HIF-2α, which promotes hypoxic cell death when induced or overexpressed in cells (12, 29, 30). It has been suggested that SDHB/D PCCs lose *BNIP3* expression via a HIF-independent pathway and that loss of *BNIP3* expression might be implicated in the increased frequency of malignant transformation reported in SDHB PCCs (16). Nevertheless, we observed that BNIP3 is also down-regulated in normal adrenal tissue, and this finding is common to all PCCs except for VHL-related tumors, suggesting that *BNIP3* down-regulation is not related to malignant behavior of SDHB PCCs. On the other hand, rather than promoting cell death, BNIP3 may allow survival by promoting autophagy (elimination of damaged mitochondria) in response to hypoxia and suppress genes required for mitochondrial biosynthesis (31, 32). This latter function of BNIP3 could explain the significant overexpression of this HIF-1α-induced molecule in the most hypoxic PCCs, which are the VHL tumors.

In summary, transcriptional profiling of a large series of PCCs/PGLs revealed unexpected EglN3 mRNA overexpression in VHL-mutated tumors compared with normal adrenal tissue and to the remaining genetic PCC classes. These high levels of EglN3 mRNA did not lead to significant differences at the protein level, so it seems that an unknown posttranscriptional mechanism should account for this discrepancy. In addition, we found that, although VHL and SDHB tumors share a common hypoxic transcriptional signature that confirms the previously described HIF regulatory loop (6), they significantly differ in the expression of major HIF-1α/HIF-2α down-

stream targets. This latter finding opens new specific therapeutic approaches for malignant PCCs taking into account the genetic background of the tumor.

Materials and Methods

Tissue specimens

Eighty-four frozen tumors from 84 unrelated patients (aged between 11 and 79 yr) were collected from different Spanish hospitals through the Spanish National Tumor Bank Network and from the Instituto Oncologico Veneto in Italy. The tissues were immediately frozen in liquid nitrogen, embedded in Tissue-Tek OCT compound (Sakura, Torrance, CA), and stored at −80 C until they were used. All tissues were evaluated by pathologists by means of hematoxylin/eosin staining; 85% was considered a suitable percentage of tumor cells per sample to be included in the study. All patients provided informed consent. In addition, medullar adrenal tissue samples from nonaffected donors were also hybridized for further comparisons.

DNA and RNA isolation

Genomic DNA and total RNA were obtained using the DNeasy (QIAGEN, Inc., Valencia, CA) and the TriReagent (MRC, Cincinnati, OH) kits, respectively, according to the manufacturers' instructions. Purity and integrity of RNA was assessed using an Agilent 2100 Bioanalyzer (Agilent Technologies, Palo Alto, CA), and degraded samples (with an RNA integrity number below 7) were discarded. Concentration was determined using a Nanodrop ND-1000 spectrophotometer.

Molecular characterization of tumors

A complete genetic characterization of five PCC susceptibility genes (*RET*, *VHL*, *SDHB*, *SDHC*, and *SDHD*) was carried out in tumor specimens and in the corresponding normal tissue, when possible (normal tissue was available for 69 out of the 84 cases). Screening for point mutations (in all genes) and gross deletions (in *VHL* and *SDHx*) was performed by direct sequencing and Multiplex Ligation-dependent Probe Amplification (MRC-Holland, Amsterdam, The Netherlands), respectively, as described (33). NF1 diagnosis was based on clinical characteristics of patients.

cDNA synthesis, labeling, hybridization, and detection

For each tumor, as well as normal adrenal tissues, 500 ng of total RNA were amplified by double strand cDNA synthesis, followed by T7-based *in vitro* transcription, according to the manufacturer's instructions. Universal Human Reference RNA (Stratagene, La Jolla, CA) was used for all samples as a reference. Amplified cRNA was then labeled with cyanine (Cy)5-conjugated 2′-deoxyuridine 5′-triphosphate, whereas cRNA from Universal Human Reference RNA was labeled with Cy3-conjugated 2′-deoxyuridine 5′-triphosphate. The Agilent Whole Human Genome platform (4x44K) was used for competitive hybridization, and the slides were washed, dried, and scanned in an Agilent microarray scanner (Agilent Technologies).

Normalization and preprocessing

Two channel ratios (Cy5/Cy3) for each array spot were generated and quantified using Feature Extraction version 9.5 software. Microarray background subtraction was carried out using the *normexp* method (34). The dataset was normalized using *loess* within-array normalization and quantile between-array normalization. Differentially expressed genes were identified by applying linear models using the Bioconductor limma R package (http://www.bioconductor.org) (35). After normalization, a preprocess step was performed by the methods implemented in the GEPAS package (36). Inconsistent replicates (SD > 1) were discarded, and consistent replicates were averaged (median method). Finally, genes that exhibited flat patterns (SD $= 0.8$) across the set of samples were filtered and omitted in further comparisons.

Unsupervised and supervised analysis

Tumor samples were grouped according to their expression profiles by means of unsupervised clustering using GeneCluster 2.0 (37). Unsupervised learning is implemented by a Self-Organizing Map algorithm and viewed in a visualizer that displays cluster profiles and relevant cluster member information. The reliability of the clusters was verified by consensus clustering, a robust clustering method which obtains the consensus across multiple runs of a clustering algorithm and assess the stability of the discovered clusters by using resampling techniques (38). This procedure performed 500 permutations to refine the cluster parameters. The most stable clusters resulting from multiple iterations were defined and used for subsequent analysis. A second unsupervised clustering of either all tumors included in the study or the SDHB- and VHL-positive cases only was performed using the expression data corresponding to a set of genes included in a recently reported ranked list of HIF target genes (39). The list of genes included 500 newly predicted and 58 well-known HIF target genes. Finally, tumors belonging to different predefined classes were used for supervised analysis to identify specific transcripts related to each genetic condition. A *t* test was carried out as implemented in POMELOII (40). To account for multiple hypothesis testing, the estimated significance level (*P*) was adjusted using Benjamini's FDR correction (41). Genes with an FDR < 0.05 were selected as differentially expressed between tumor classes.

Functional profile analysis

To discover biological processes differentially regulated between the genetic classes, we employed GSEA (42) using BioCarta and Kyoto Encyclopedia of Genes and Genomes annotations. Gene expression values were ranked based on *t* statistic for Kolmogorov-Smirnoff testing. GSEA yields a normalized enrichment score that represents the degree of enrichment of the gene set in the ranked gene list, and a *P* (NOM *P*) that measures the significance of that score. To account for multiple testing, the NOM *P* was adjusted using FDR. Those gene sets showing FDR < 0.25 were considered enriched between classes under comparison.

Validation of microarray data by quantitative real-time RT-PCR

To validate microarray data, expression levels of selected significantly differentially expressed genes were assessed by RT-PCR in 13 of the 84 previously hybridized samples and in 13 FFPE tumors from an independent series. Reverse transcription was performed using 1 μg total RNA, random hexamers, and M-MLV Reverse Transcriptase (Promega Corp., Madison, WI). PCRs were done on an ABI Prism 7000 sequence detection sys-

tem (Applied Biosystems, Foster City, CA) using the Universal ProbeLibrary set (Roche Applied Science, Indianapolis, IN) as described by the manufacturer. All analyses were performed in triplicate, and relative RNA levels were determined using hypoxanthine phosphoribosyltransferase 1-RNA as internal control. The Mann-Whitney test was used to compare the two genetic classes.

Immunohistochemistry

Immunohistochemical staining was performed using 3-μm FFPE sections included in two tissue microarrays. The microarrays contained PCCs/PGLs from patients carrying different germline mutations: eight in *VHL*, 10 in *SDHB*, 24 in *RET*, and for in *SDHD*. Nine sporadic cases and three normal adrenal sections were included as controls. Slides were processed by means of a standard protocol using EglN3 (mouse monoclonal 188E, kindly provided by Patrick J. Pollard), HIF-1α (mouse monoclonal antibody; Abcam, Cambridge, MA), and HIF-2α (rabbit polyclonal; Novus Biologicals, Littleton, CO) primary antibodies and the Envision System (Dako, Carpinteria, CA) for antigen-antibody detection. Regarding EglN3 subcellular localization, we only considered staining in the cytoplasm, and when positive, 100% of cells were found to be stained. We delineated four levels of staining: 0 (null staining), 1 (low staining), 2 (medium staining), and 3 (strong staining), which we grouped into negative (0), midlevel (1 and 2), and positive (3).

Methylation-specific polymerase chain reaction (MSP)

The methylation status of *EglN3* CpG islands was analyzed using the MSP technique (43). Normal lymphocytes and *in vitro*-methylated DNA were used as positive controls for the unmethylated and methylated sequences, respectively. In selected samples, methylation status was confirmed by bisulfite genomic sequencing, as described (44). The primers used for the MSP analysis are available on request.

Acknowledgments

A.C. and C.R.-A. hold Fondo de Investigación Sanitaria and "Ramon y Cajal" contracts, respectively, from the Spanish government, and I.M. holds a Caja Navarra contract. Tissue samples were provided by both the Tumor Bank Network founded by the Molecular Pathology Program of the Spanish National Cancer Centre and the Regional Network of Tumor Banks of Castilla y León.

Address all correspondence and requests for reprints to: Alberto Cascón, Ph.D., Hereditary Endocrine Cancer Group, Human Cancer Genetics Programme. Centro Nacional de Investigaciones Oncológicas, Melchor Fernández Almagro 3, 28029 Madrid, Spain. E-mail: acascon@cnio.es; or Mercedes Robledo, Ph.D. E-mail: mrobledo@cnio.es.

This work was supported in part by Fondo de Investigaciones Sanitarias Projects PI061477 (to A.C.) and PI080883 (to M.R.), Fundación Mutua Madrileña (M.R.), and the Spanish Ministry of Science and Innovation Project Intramural-706-2 Instituto de Salud Carlos III Center for Biomedical Research on Rare Diseases.

Disclosure Summary: The authors have nothing to disclose.

References

1. **Hao HX, Khalimonchuk O, Schraders M, Dephoure N, Bayley JP, Kunst H, Devilee P, Cremers CW, Schiffman JD, Bentz BG, Gygi SP, Winge DR, Kremer H, Rutter J** 2009 SDH5, a gene required for flavination of succinate dehydrogenase, is mutated in paraganglioma. Science 325:1139–1142
2. **Burnichon N, Brière JJ, Libé R, Vescovo L, Rivière J, Tissier F, Jouanno E, Jeunemaitre X, Bénit P, Tzagoloff A, Rustin P, Bertherat J, Favier J, Gimenez-Roqueplo AP** 2010 SDHA is a tumor suppressor gene causing paraganglioma. Hum Mol Genet 19:3011–3020
3. **Qin Y, Yao L, King EE, Buddavarapu K, Lenci RE, Chocron ES, Lechleiter JD, Sass M, Aronin N, Schiavi F, Boaretto F, Opocher G, Toledo RA, Toledo SP, Stiles C, Aguiar RC, Dahia PL** 2010 Germline mutations in TMEM127 confer susceptibility to pheochromocytoma. Nat Genet 42:229–233
4. **Lee S, Nakamura E, Yang H, Wei W, Linggi MS, Sajan MP, Farese RV, Freeman RS, Carter BD, Kaelin Jr WG, Schlisio S** 2005 Neuronal apoptosis linked to EglN3 prolyl hydroxylase and familial pheochromocytoma genes: developmental culling and cancer. Cancer Cell 8:155–167
5. **Schlisio S, Kenchappa RS, Vredeveld LC, George RE, Stewart R, Greulich H, Shahriari K, Nguyen NV, Pigny P, Dahia PL, Pomeroy SL, Maris JM, Look AT, Meyerson M, Peeper DS, Carter BD, Kaelin Jr WG** 2008 The kinesin KIF1Bβ acts downstream from EglN3 to induce apoptosis and is a potential 1p36 tumor suppressor. Genes Dev 22:884–893
6. **Dahia PL, Ross KN, Wright ME, Hayashida CY, Santagata S, Barontini M, Kung AL, Sanso G, Powers JF, Tischler AS, Hodin R, Heitritter S, Moore F, Dluhy R, Sosa JA, Ocal IT, Benn DE, Marsh DJ, Robinson BG, Schneider K, Garber J, Arum SM, Korbonits M, Grossman A, Pigny P, Toledo SP, Nosé V, Li C, Stiles CD** 2005 A HIF1α regulatory loop links hypoxia and mitochondrial signals in pheochromocytomas. PLoS Genet 1:72–80
7. **Eisenhofer G, Huynh TT, Pacak K, Brouwers FM, Walther MM, Linehan WM, Munson PJ, Mannelli M, Goldstein DS, Elkahloun AG** 2004 Distinct gene expression profiles in norepinephrine- and epinephrine-producing hereditary and sporadic pheochromocytomas: activation of hypoxia-driven angiogenic pathways in von Hippel-Lindau syndrome. Endocr Relat Cancer 11:897–911
8. **Favier J, Brière JJ, Burnichon N, Rivière J, Vescovo L, Benit P, Giscos-Douriez I, De Reyniès A, Bertherat J, Badoual C, Tissier F, Amar L, Libé R, Plouin PF, Jeunemaitre X, Rustin P, Gimenez-Roqueplo AP** 2009 The Warburg effect is genetically determined in inherited pheochromocytomas. PLoS One 4:e7094
9. **Gimenez-Roqueplo AP, Favier J, Rustin P, Rieubland C, Crespin M, Nau V, Khau Van Kien P, Corvol P, Plouin PF, Jeunemaitre X** 2003 Mutations in the SDHB gene are associated with extra-adrenal and/or malignant phaeochromocytomas. Cancer Res 63:5615–5621
10. **Brouwers FM, Eisenhofer G, Tao JJ, Kant JA, Adams KT, Linehan WM, Pacak K** 2006 High frequency of SDHB germline mutations in patients with malignant catecholamine-producing paragangliomas: implications for genetic testing. J Clin Endocrinol Metab 91:4505–4509
11. **Adjallé R, Plouin PF, Pacak K, Lehnert H** 2009 Treatment of malignant pheochromocytoma. Horm Metab Res 41:687–696
12. **Raval RR, Lau KW, Tran MG, Sowter HM, Mandriota SJ, Li JL, Pugh CW, Maxwell PH, Harris AL, Ratcliffe PJ** 2005 Contrasting properties of hypoxia-inducible factor 1 (HIF-1) and HIF-2 in von Hippel-Lindau-associated renal cell carcinoma. Mol Cell Biol 25:5675–5686
13. **Chen C, Pore N, Behrooz A, Ismail-Beigi F, Maity A** 2001 Regulation of glut1 mRNA by hypoxia-inducible factor-1. Interaction between H-ras and hypoxia. J Biol Chem 276:9519–9525
14. **Gustafsson MV, Zheng X, Pereira T, Gradin K, Jin S, Lundkvist J, Ruas JL, Poellinger L, Lendahl U, Bondesson M** 2005 Hypoxia

requires notch signaling to maintain the undifferentiated cell state. Dev Cell 9:617–628
15. **Maranchie JK, Zhan Y** 2005 Nox4 is critical for hypoxia-inducible factor 2-α transcriptional activity in von Hippel-Lindau-deficient renal cell carcinoma. Cancer Res 65:9190–9193
16. **Pollard PJ, El-Bahrawy M, Poulsom R, Elia G, Killick P, Kelly G, Hunt T, Jeffery R, Seedhar P, Barwell J, Latif F, Gleeson MJ, Hodgson SV, Stamp GW, Tomlinson IP, Maher ER** 2006 Expression of HIF-1α, HIF-2α (EPAS1), and their target genes in paraganglioma and pheochromocytoma with VHL and SDH mutations. J Clin Endocrinol Metab 91:4593–4598
17. **Cervera AM, Apostolova N, Crespo FL, Mata M, McCreath KJ** 2008 Cells silenced for SDHB expression display characteristic features of the tumor phenotype. Cancer Res 68:4058–4067
18. **Lee CM, Hickey MM, Sanford CA, McGuire CG, Cowey CL, Simon MC, Rathmell WK** 2009 VHL Type 2B gene mutation moderates HIF dosage in vitro and in vivo. Oncogene 28:1694–1705
19. **Aprelikova O, Chandramouli GV, Wood M, Vasselli JR, Riss J, Maranchie JK, Linehan WM, Barrett JC** 2004 Regulation of HIF prolyl hydroxylases by hypoxia-inducible factors. J Cell Biochem 92:491–501
20. **Jaakkola P, Mole DR, Tian YM, Wilson MI, Gielbert J, Gaskell SJ, Kriegsheim Av, Hebestreit HF, Mukherji M, Schofield CJ, Maxwell PH, Pugh CW, Ratcliffe PJ** 2001 Targeting of HIF-α to the von Hippel-Lindau ubiquitylation complex by O2-regulated prolyl hydroxylation. Science 292:468–472
21. **Kaelin Jr WG** 2008 The von Hippel-Lindau tumour suppressor protein: O_2 sensing and cancer. Nat Rev Cancer 8:865–873
22. **Berra E, Benizri E, Ginouvès A, Volmat V, Roux D, Pouysségur J** 2003 HIF prolyl-hydroxylase 2 is the key oxygen sensor setting low steady-state levels of HIF-1α in normoxia. EMBO J 22:4082–4090
23. **Fu J, Menzies K, Freeman RS, Taubman MB** 2007 EGLN3 prolyl hydroxylase regulates skeletal muscle differentiation and myogenin protein stability. J Biol Chem 282:12410–12418
24. **Fu J, Taubman MB** 2010 Prolyl hydroxylase EGLN3 regulates skeletal myoblast differentiation through an NF-κB-dependent pathway. J Biol Chem 285:8927–8935
25. **Xue J, Li X, Jiao S, Wei Y, Wu G, Fang J** 2010 Prolyl hydroxylase-3 is down-regulated in colorectal cancer cells and inhibits IKKβ independent of hydroxylase activity. Gastroenterology 138:606–615
26. **Sato E, Torigoe T, Hirohashi Y, Kitamura H, Tanaka T, Honma I, Asanuma H, Harada K, Takasu H, Masumori N, Ito N, Hasegawa T, Tsukamoto T, Sato N** 2008 Identification of an immunogenic CTL epitope of HIFPH3 for immunotherapy of renal cell carcinoma. Clin Cancer Res 14:6916–6923
27. **Steenhard BM, Isom K, Stroganova L, St John PL, Zelenchuk A, Freeburg PB, Holzman LB, Abrahamson DR** 2010 Deletion of Von Hippel-Lindau in glomerular podocytes results in glomerular basement membrane thickening, ectopic subepithelial deposition of collagen $\alpha1\alpha2\alpha1$(IV), expression of neuroglobin, and proteinuria. Am J Pathol 177:84–96
28. **Hatzimichael E, Dasoula A, Shah R, Syed N, Papoudou-Bai A, Coley HM, Dranitsaris G, Bourantas KL, Stebbing J, Crook T** 2010 The prolyl-hydroxylase EGLN3 and not EGLN1 is inactivated by methylation in plasma cell neoplasia. Eur J Haematol 84:47–51
29. **Kothari S, Cizeau J, McMillan-Ward E, Israels SJ, Bailes M, Ens K, Kirshenbaum LA, Gibson SB** 2003 BNIP3 plays a role in hypoxic cell death in human epithelial cells that is inhibited by growth factors EGF and IGF. Oncogene 22:4734–4744
30. **Fei P, Wang W, Kim SH, Wang S, Burns TF, Sax JK, Buzzai M, Dicker DT, McKenna WG, Bernhard EJ, El-Deiry WS** 2004 Bnip3L is induced by p53 under hypoxia, and its knockdown promotes tumor growth. Cancer Cell 6:597–609
31. **Kaelin Jr WG** 2009 SDH5 mutations and familial paraganglioma: somewhere Warburg is smiling. Cancer Cell 16:180–182
32. **Tracy K, Dibling BC, Spike BT, Knabb JR, Schumacker P, Macleod KF** 2007 BNIP3 is an RB/E2F target gene required for hypoxia-induced autophagy. Mol Cell Biol 27:6229–6242
33. **Cascon A, Pita G, Burnichon N, Landa I, Lopez-Jimenez E, Montero-Conde C, Leskela S, Leandro-Garcia LJ, Leton R, Rodriguez-Antona C, Diaz JA, Lopez-Vidriero E, Gonzalez-Neira A, Velasco A, Matias-Guiu X, Gimenez-Roqueplo AP, Robledo M** 2009 Genetics of pheochromocytoma and paraganglioma in Spanish patients. J Clin Endocrinol Metab 94:2677–2683
34. **Ritchie ME, Silver J, Oshlack A, Holmes M, Diyagama D, Holloway A, Smyth GK** 2007 A comparison of background correction methods for two-colour microarrays. Bioinformatics 23:2700–2707
35. **Smyth GK, Michaud J, Scott HS** 2005 Use of within-array replicate spots for assessing differential expression in microarray experiments. Bioinformatics 21:2067–2075
36. **Montaner D, Tárraga J, Huerta-Cepas J, Burguet J, Vaquerizas JM, Conde L, Minguez P, Vera J, Mukherjee S, Valls J, Pujana MA, Alloza E, Herrero J, Al-Shahrour F, Dopazo J** 2006 Next station in microarray data analysis: GEPAS. Nucleic Acids Res 34:W486–W491
37. **Reich M, Ohm K, Angelo M, Tamayo P, Mesirov JP** 2004 GeneCluster 2.0: an advanced toolset for bioarray analysis. Bioinformatics 20:1797–1798
38. **Monti S, Tamayo P, Mesirov J, Golub T** 2003 Consensus clustering: a resampling-based method for class discovery and visualization of gene expression microarray data. Mach Learn 52:91–118
39. **Benita Y, Kikuchi H, Smith AD, Zhang MQ, Chung DC, Xavier RJ** 2009 An integrative genomics approach identifies hypoxia inducible factor-1 (HIF-1)-target genes that form the core response to hypoxia. Nucleic Acids Res 37:4587–4602
40. **Morrissey ER, Diaz-Uriarte R** 2009 Pomelo II: finding differentially expressed genes. Nucleic Acids Res 37(Suppl 2): W581–W586
41. **Benjamini Y, Drai D, Elmer G, Kafkafi N, Golani I** 2001 Controlling the false discovery rate in behavior genetics research. Behav Brain Res 125:279–284
42. **Subramanian A, Tamayo P, Mootha VK, Mukherjee S, Ebert BL, Gillette MA, Paulovich A, Pomeroy SL, Golub TR, Lander ES, Mesirov JP** 2005 Gene set enrichment analysis: a knowledge-based approach for interpreting genome-wide expression profiles. Proc Natl Acad Sci USA 102:15545–15550
43. **Herman JG, Graff JR, Myöhänen S, Nelkin BD, Baylin SB** 1996 Methylation-specific PCR: a novel PCR assay for methylation status of CpG islands. Proc Natl Acad Sci USA 93:9821–9826
44. **Esteller M, Sparks A, Toyota M, Sanchez-Cespedes M, Capella G, Peinado MA, Gonzalez S, Tarafa G, Sidransky D, Meltzer SJ, Baylin SB, Herman JG** 2000 Analysis of adenomatous polyposis coli promoter hypermethylation in human cancer. Cancer Res 60:4366–4371